

Electrochemical and Dissolution Behavior of the Ti-alloy VT-9 in H₂SO₄ Solution in the Presence of the Organic Inhibitor (2-Phenyl-4-[(E)-1-(4-solphanylanilino)methyliden]-1,3-oxazole-5(4H)-one

S.M.A. Hosseini* and M. Amiri

Dept. of Chemistry, Faculty of Science, Shahid Bahonar University of Kerman, 76169, Kerman, Iran

(Received 28 May 2006, Accepted 20 March 2007)

This investigation potentiodynamically evaluates the corrosion behavior of a high strength titanium alloy, VT-9, in 4 M sulfuric acid solution containing different concentrations (10, 20, 30 ppm) of the organic inhibitor, 2-phenyl-4-[(E)-1-(4-sulfanylanilino)methylidene]-1,3-oxazole-5(4H)-one (L-SH), at different temperatures (293, 303 and 313 ± 1 K). The open circuit potential values noted before and after each experiment varied appreciably with time. These values, in the presence of L-SH, were negative before polarization, but after completion of the experiment turned positive and remained stable over a long period of time. The cathodic current density values increased with increasing cathodic potential (more negative). The corrosion potential (E_{corr}) increased remarkably with the addition of L-SH. The corrosion current densities (I_{corr}), critical current density (I_{cr}), and passive current density (I_{p}) all decreased when L-SH was used. However, only the decrease in the I_{corr} with increasing amounts of inhibitor was significant compared to that of I_{cr} and I_{p} . L-SH expanded the range of the passive potential. SEM micrographs and open circuit potential measurements revealed the formation of a uniform and protective film on the alloy surface in the presence of L-SH, which acted as an efficient inhibitor.

Keywords: Ti alloy, Corrosion, Organic compound, Inhibitor

INTRODUCTION

For scientific and technical progress in industries, the use of various aggressive work media is integral, as is a wide use of new materials. Among these, titanium and its alloys are successful in competing with the main structural metals, including steels, non-ferrous metal alloys and aluminum. Titanium and its alloys are being used in the food industry [1], desalination plants [2], as well as in restorative implements such as dental and orthopedic prostheses, pacemakers and heart valves [3], due to their appropriate mechanical properties, excellent corrosion resistance in biological fluids, and biocompatibility [4]. However, Ti materials are

susceptible to many forms of corrosion. For example, although not widely known, localized preferential corrosion in the welded areas of titanium and Ti alloys used in the chemical processing industry results in perforation caused by pitting corrosion [5]. The instability of Ti and its alloys in reducing acid solutions has been identified and has drawn the attention of researchers toward the study of the electrochemical behavior of Ti in acidic media [6,7]. Titanium alloys that consist of only alpha phase are commonly used in industrial applications where corrosion resistance is a primary concern. However, the recently developed Ti alloy, VT-9, exhibits relatively good corrosion resistance, due to the formation of titania (TiO₂) on its surface. The nature, composition and thickness of these protective oxide scales depend on the environmental conditions [8]. Furthermore, corrosion is often

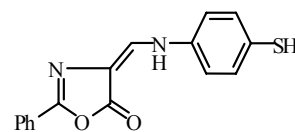
*Corresponding author. E-mail: s.m.a.hosseini@mail.uk.ac.ir

controlled by adding inhibitors into these media. Corrosion inhibitors may be classified as oxidizing, precipitation and adsorption inhibitors [9]. Adsorption inhibitors, organic substances displaying polar functions with nitrogen, sulfur and/or oxygen in the conjugated system [10,11]. Adsorption inhibitors are known to work by attaching to the surface of a metal *via* metal ions in the lattice, which slow the dissolution of the metal by virtue of adsorption, using the polar group as the reaction center for the adsorption process [12,13]. The strength of the adsorption bond depends on the makeup of the metal and corrosive material, the structure and concentration of the inhibitor, as well as the temperature [14]. Inhibitor molecules may physically or chemically adsorb onto the metal surface. Physisorbed molecules adhere to the metal at local cathodes and slow metal dissolution by inhibiting the cathodic reaction. Chemisorbed molecules, on the other hand, shield anodic areas, reducing the reactivity of the metal at the attachment sites [15,16]. The more efficient inhibitors preferentially protect anodic areas by chemisorption [9]. Brynza and Gerasyutina, [17,18] while investigating the corrosion resistance of Ti in certain applications in the chemical industry, have studied organic inhibitors in sulfuric acid and hydrochloric acid. Most organic inhibitors, used to protect titanium against corrosion, function as oxidizers that are principally reduced on the metal surface, thus enhancing the effectiveness of the cathodic process [19]. Very few corrosion studies have been reported for the alloy VT-9 in sulfuric acid, in spite of its commercial importance in various industries, where it is used to replace Ti, since it meets the strength requirement. The present investigation studies the inhibition behavior of VT-9 in 4 M sulfuric acid in the presence of different concentrations (10, 20 and 30 ppm) of the organic compound 2-phenyl-4-[(E)-1-(4-sulfanylanilino)methylidene]-1,3-oxazole-5(4H)-one (hereafter referred to as L-SH, as shown in Scheme 1) at various temperatures. Inhibitory characteristics are determined using open circuit potential (OCP) measurements, potentiodynamic scanning and scanning electron microscopy (SEM).

EXPERIMENTAL

Material and Chemicals

A cylinder made of VT-9, composed of a Ti matrix



Scheme 1. Structure of L-SH

containing 5.47% Al, 2.9% Mo, 1.9% Zr and 0.22% Si, was cut into pieces, each with a surface area of 2 cm², and used as working electrodes. Prior to immersion in the electrolyte, the individual specimens were mechanically polished with different grades (400, 800, 1200, and 1500 grit) of emery paper. After polishing, the specimens were etched in an aqueous mixture of HF and HNO₃ (2/4 volume ratio) for a few seconds at room temperature to remove any possible oxide film, and then washed with double distilled water. The specimens were finally degreased with acetone. A platinum electrode and a saturated calomel electrode (SCE) were used as counter and reference electrodes, respectively. Potentiodynamic polarization studies were performed in 4 M H₂SO₄ containing various concentrations of L-SH (10, 20 and 30 ppm).

Preparation of L-SH

A mixture of hippuric acid (18 g, 0.1 mmol), triethylorthoformate (14.0 g, 0.09 mmol) and acetic anhydride (20 ml, 0.21 mmol) was heated at 140 °C for 1 h. The solvents were removed *in vacuo*, the residue dissolved in 25 ml of alcohol, cooled, filtered and then washed with cold petroleum ether to give 2-phenyl-4-(ethoxymethylene)-5(4H)-oxazolone (70%). To a solution of 2-phenyl-4-(ethoxymethylene)-5(4H)-oxazolone (0.43 g, 2.0 mmol) in 50 ml of dry benzene, 0.25 g (2.0 mmol) of 4-amiothiophenol and 0.2 ml of triethylamine was added. The mixture was stirred for 5 h at room temperature, then filtered and washed with dry benzene. The residue was recrystallized from ethanol (96%), giving 0.47 g of yellow crystals (yield 77%), m.p.: 174 °C. The structure of the product was determined by spectroscopic methods (IR, NMR, and MS) and elemental analyses for C, H, and N.

Apparatus and Procedures

The electrochemical measurements were performed using

a potentiostat CG (CV & PG system model DPSWx). Prior to polarization measurement, the Ti-alloy working electrode was immersed in the experimental solution for ~30 min to attain a stable OCP value. Polarization was performed moving from negative to positive potentials in the range of -800 to 1600 mV, with a scan rate of 1 mV s⁻¹, at constant temperatures (within ±1 K of the target value). The influence of temperature was investigated at 293, 303 and 313 ± 1 K for each concentration of inhibitor. All potentials were measured against the SCE. The corrosion parameters, including the corrosion potential (E_{corr}), corrosion current densities (I_{corr}), cathodic Tafel slopes (β_c), and inhibition efficiency (% η), were used to evaluate the corrosion behavior of the alloy in the test solution. Micrographs were obtained using an SEM model CamScan MV 2300.

RESULTS AND DISCUSSION

The potentiodynamic polarization curves of VT-9 in sulfuric acid with different concentrations of L-SH at different temperatures are shown in Figs. 1-3. Here, we observe that the specimens undergo an active-to-passive transition in all the experimental solutions. The shape and nature of these curves are similar to those previously reported for Ti and its alloys in reducing acids [20,21]. For the blank solution, the OCP of the sample before polarization was -580 mV vs. SCE, followed by 320 mV vs. SCE after polarization, and then -200 mV vs. SCE after 24 h. This value (-200 mV vs. SCE) gradually dropped to -500 mV vs. SCE and finally attained a stable value of -570 mV vs. SCE.

Note that in 4 M acid in the presence of 10, 20 and 30 ppm L-SH at 303 K, before polarization the OPC occurs between -270 and -80 mV vs. SCE. However, after polarization the OCP values range from 390 to 570 mV vs. SCE. The increase in the value of the OCP after polarization is due to the passive formation of a film on the surface of the samples.

From Fig. 4, the measurement of the OCP value over time reveals that after 24 h the film remained protective during the prolonged exposure to the acid solution containing 30 ppm L-SH at 303 ± 1 K. The OCP value decreased slightly after further exposure and thereafter was stable. This suggests that the insulating properties of the film formed on the surface did not change, even if the anodic film had dissolved to some

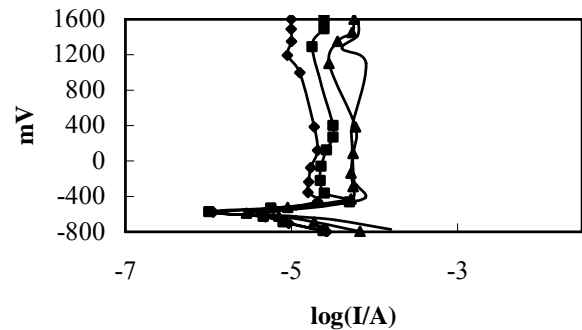


Fig. 1. Polarization curves of VT-9 in 4 M sulfuric acid + L-SH at 293 ± 1 K: (—) blank, (▲) 10 ppm, (■) 20 ppm, (◆) 30 ppm.

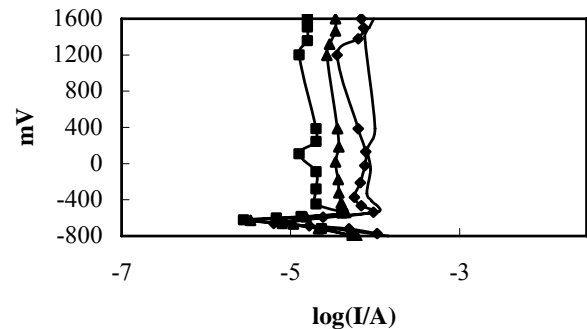


Fig. 2. Polarization curves of VT-9 in 4 M sulfuric acid + L-SH at 303 ± 1 K: (—) blank, (◆) 10 ppm, (▲) 20 ppm, (■) 30 ppm.

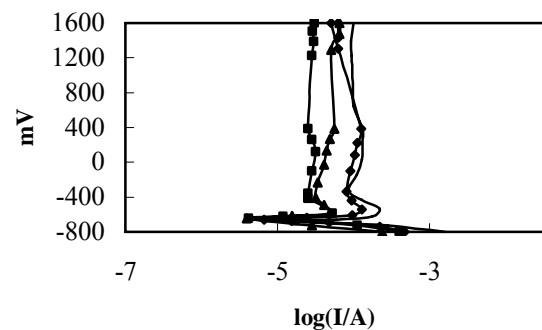


Fig. 3. Polarization curves of VT-9 in 4 M sulfuric acid + L-SH at 313 ± 1 K: (—) blank, (◆) 10 ppm, (▲) 20 ppm, (■) 30 ppm.

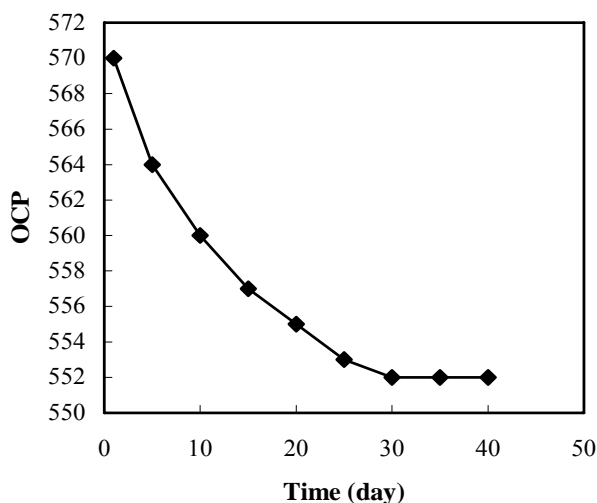


Fig. 4. OCP values vs. time in the presence of 30 ppm L-SH at 303 ± 1 K.

extent at OCP.

The cathodic curves, in general, are almost similar. This similarity suggests that a similar cathodic reaction is occurring on the surface of the electrode, regardless of the concentration of L-SH. Where metal dissolution is the anodic reaction, the possible cathodic reaction is either the reduction of oxygen or water in a neutral solution [22], or proton reduction in an acidic solution. The corrosion parameters obtained from the polarization curves are listed in Tables 1-3. In the present investigation, the cathodic Tafel slopes derived from the curves were found to be in the range of 110-140 mV per decade of current vs. SCE. These values are consistent with previously reported values for the evolution of hydrogen [23]. The percentage inhibition efficiency ($\% \eta$) and surface coverage degree (θ) are obtained from the following equations [24]:

$$\eta = \left(\frac{i_0 - i_1}{i_0} \right) \times 100\%, \quad \theta = \left(\frac{i_0 - i_1}{i_0} \right)$$

where, i_0 and i_1 are the corrosion current densities obtained in the absence and presence of the inhibitor. It is observed that the E_{corr} shifts toward the noble direction (increase) in the presence of the inhibitor. The corrosion current density I_{corr} ,

critical current density I_{cr} and passive current density I_{p} decrease as the concentration of L-SH increases, but the corrosion potentials E_{corr} increase. An overall examination of the polarization curves in Figs. 1-3 show that the anodic curves at different temperatures are similar in nature. However, the corrosion potential shifted toward more active potentials with increasing temperature, but current densities (I_{cr} , I_{p}) increased as the temperature increased from 293 to 313 ± 1 K. In the presence of 30 ppm L-SH, the corrosion current did not increase from 303 K to 313 K, but, because of the difference in the I_{corr} blank, inhibition efficiency increased. The active dissolution range increased with temperature. The broadly similar curves at different temperatures suggest similar reactions at the surface of the electrode, but with different rates. The percentage inhibition efficiency ($\% \eta$) and surface coverage degree (θ) increased with increasing inhibitor concentration, that implies strong adsorption of this inhibitor on the surface of alloy. The percentage inhibition efficiency was higher at 30 ppm of L-SH at 313 K compared to 293 and 303 K. The nature of the inhibitor interaction on the corroding surface during corrosion inhibition of metals and alloys has been deduced in terms of adsorption characteristics of the inhibitor. The surface coverage (θ) data are very useful while discussing the adsorption characteristics [24]. According to Ebenso [25] and Al-Mayouf [26] a decrease in the inhibition efficiency with a rise in temperature suggests that inhibitor molecules are physically adsorbed on the metal surface while the reverse behavior suggests chemisorption. The reason for this behavior is still not quite clear and several factors may possibly play a role for this behavior. The orientation of adsorbed aromatics is a function of several variables, among which are adsorbate molecular structure and solute concentration, and the reactivity of these adsorbed intermediates is a sensitive function of their orientation [27]. Generally, the mechanism by which a given inhibitor may attach to metal depends on the functional group present in its molecule. Some functional groups are normally held more firmly than others [28]. According to Fragnani and Trabonelli [29], sulfur-containing substances easily chemisorb onto the surface of metal in acid media, whereas nitrogen-containing compounds tend to favor physisorption. This suggestion has been corroborated by the results of other authors [30]. Thus, for inhibitors containing both sulfur and nitrogen, at lower

Electrochemical and Dissolution Behavior of the Ti-alloy VT-9

Table 1. Corrosion Parameters of VT-9 in 4 M Sulfuric Acid in the Presence of LS-H at 293 ± 1 K

Concentration of L-SH (ppm)	E_{corr} (mV)	I_{corr} (A cm ⁻²)	I_{cr} (A cm ⁻²)	E_p (mV)	I_p (A cm ⁻²)	$\eta\%$	θ
Blank	-575	3.9×10^{-5}	7.6×10^{-5}	-281	6.1×10^{-5}		
10	-562	2.8×10^{-5}	5.2×10^{-5}	-311	4.5×10^{-5}	28	0.28
20	-544	1.9×10^{-5}	4.3×10^{-5}	-324	2.6×10^{-5}	51	0.51
30	-525	1.1×10^{-5}	1.8×10^{-5}	-330	0.9×10^{-5}	71	0.71

Table 2. Corrosion Parameters of VT-9 in 4 M Sulfuric Acid in the Presence of LS-H at 303 ± 1 K

Concentration of L-SH (ppm)	E_{corr} (mV)	I_{corr} (A cm ⁻²)	I_{cr} (A cm ⁻²)	E_p (mV)	I_p (A cm ⁻²)	$\eta\%$	θ
Blank	-680	7.7×10^{-5}	9.2×10^{-5}	-416	8.0×10^{-5}		
10	-662	6.3×10^{-5}	7.8×10^{-5}	-435	5.7×10^{-5}	18	0.18
20	-634	4.6×10^{-5}	5.5×10^{-5}	-449	3.7×10^{-5}	40	0.40
30	-625	1.2×10^{-5}	5.3×10^{-5}	-464	2.4×10^{-5}	84	0.84

Table 3. Corrosion Parameters of VT-9 in 4 M Sulfuric Acid in the Presence of LS-H at 313 ± 1 K

Concentration of L-SH (ppm)	E_{corr} (mV)	I_{corr} (A cm ⁻²)	I_{cr} (A cm ⁻²)	E_p (mV)	I_p (A cm ⁻²)	$\eta\%$	θ
Blank	-730	8.1×10^{-5}	9.8×10^{-5}	-400	7.5×10^{-5}		
10	-712	6.8×10^{-5}	7.9×10^{-5}	-445	5.7×10^{-5}	16	0.16
20	-694	5.0×10^{-5}	6.5×10^{-5}	-459	3.7×10^{-5}	38	0.38
30	-685	1.2×10^{-5}	5.7×10^{-5}	-464	2.9×10^{-5}	86	0.86

concentrations the adsorbed molecules are oriented with the nitrogen atom functioning as the reaction center for the adsorption process, and, as the concentration increases, reorientation of adsorbed molecules takes place, and the sulfur atom becomes the anchor. This behavior is consistent with the earlier suggestion by Shaw [31] that a molecule may first physically adsorb and then slowly react with the metal surface to form a chemisorbed layer. Thus, L-SH, having sulfur and nitrogen atoms, functions by a dual inhibitory mechanism and,

depending on the concentration, inhibits both cathodic and anodic reactions.

Figure 5 and Table 4 show that L-SH is physically adsorbed at low concentrations, however, at high concentrations (30 ppm), the inhibitor molecules are easily chemisorbed on the metal surface. The corrosion reaction may be regarded as an Arrhenius-type process and its rate is given by:

$$I_{corr} = \kappa \exp(-E_a/RT)$$

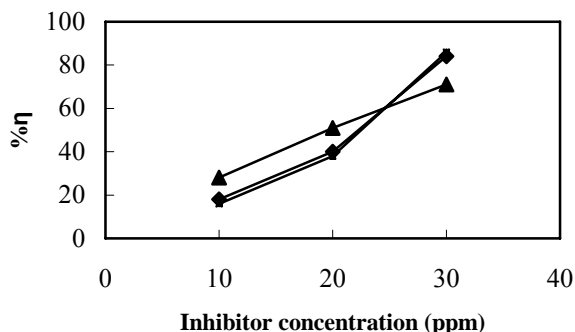


Fig. 5. Variation of inhibition efficiency with inhibitor concentration at different temperatures: (▲) 293 K, (◆) 303 K, (■) 313 K.

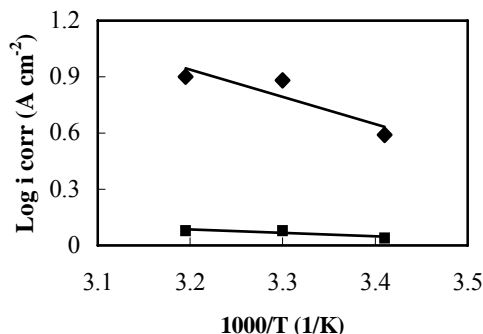


Fig. 6. Arrhenius slopes calculated from corrosion current density for Ti-alloy in the absence and presence of L-SH: (◆) blank, (■) 30 ppm L-SH.

Table 4. The Effect of Temperature on the Inhibition Efficiency of L-SH

Inhibitor concentration (ppm)	Inhibition efficiency (%)		
	293 K	303 K	313 K
10	28	18	16
20	51	40	38
30	71	84	86

where, κ is the Arrhenius pre-exponential constant, and E_a is the activation corrosion energy for the corrosion process. Figure 6 presents the Arrhenius plots of the logarithm of the corrosion current density (i_{corr}) vs. $1000/\text{temperature (T)}$ in degrees Kelvin, for the alloy, in the presence and absence of 30 ppm L-SH. The E_a values were determined from the slopes of these curves and are calculated to be $12.06 \text{ kJ mol}^{-1}$ and 1.52 kJ mol^{-1} in the absence and presence of 30 ppm L-SH. The apparent activation energy obtained for the alloy in this media is considered to be associated with the complex process/mechanism/resistance/dissolution that occurs in this region [21].

Figure 7 shows the surface of the alloy in the blank media (4 M acid without L-SH). Here, we observe that the surface of the alloy is of dual phase and is possibly covered with a very thin film. The alloy is an $\alpha+\beta$ -type, where Al is the stronger α stabilizer, Mo is the β stabilizer and Zr is almost neutral. Therefore, the alloying elements have been added to titanium

to develop a dual phase structure. Alloying elements have been reported to increase the resistance of a metal to one corrosive medium but decrease its resistance to another [32].

The micrograph in Fig. 8 shows the surface of the alloy in acid solution in the presence of L-SH. The surface of the sample is clearly covered with a uniform film of small grains.

For an inhibitor to have a high surface coverage, a chemical bond between the inhibitor should bond to the metal atom more strongly than to the molecules of the medium. The corrosion inhibitors adsorb to the metal surface atoms at the metal/solution interface through electrostatic or covalent bonding. The planarity (π) and lone pair of electrons present on heteroatom are the important structured features that determine the adsorption of these molecules on the metal surface. The π -electrons of the double bond form a chemical bond with the d-orbital of transition metals [33] thereby inhibiting corrosion. At the same time, both π -electrons and lone pair of electrons present on nitrogen, sulfur and oxygen

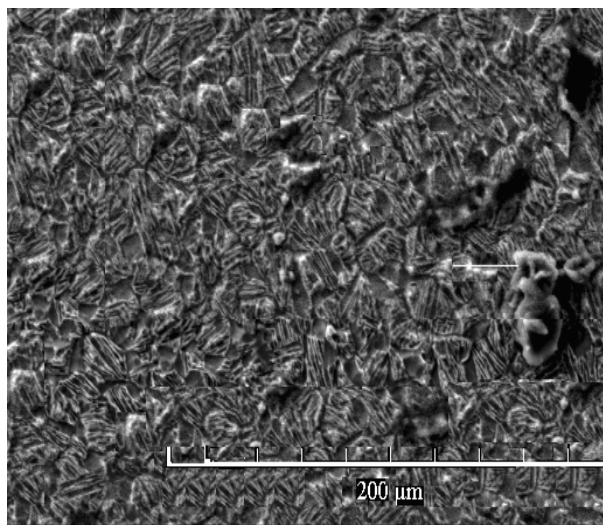


Fig. 7. SEM micrograph of the surface of alloy in 4 M sulfuric acid.

of L-SH play an important role in the adsorption of inhibitor onto the metal surface.

CONCLUSIONS

The potentiodynamic polarization curves of VT-9 in sulfuric acid with and without inhibitor exhibited an active-to-passive transition state. The inhibitor had a statistically significant influence on corrosion resistance, in terms of E_{corr} , I_{corr} and I_p of the alloy. Increasing the inhibitor concentration leads to an increase in the corrosion resistance, with lower values for I_{corr} and I_p , and a steeper cathodic Tafel slope. Furthermore, L-SH acts as a cathodic and anodic inhibitor, and belongs to the group of inhibitors classified as passivators.

Its adsorption to the Ti surface may be the main reason for the passivation of the Ti alloy. The passivated alloy remained stable, even over prolonged exposure in the presence of 30 ppm L-SH in acidic media under open circuit conditions, and transpassivity behavior was not observed. The inhibition of corrosion of the Ti alloy in H_2SO_4 by L-SH is attributed to the adsorption of this inhibitor onto the alloy surface *via* double bonding of carbon atoms and lone pair electrons present on the nitrogen, sulfur and oxygen in the conjugated system. The

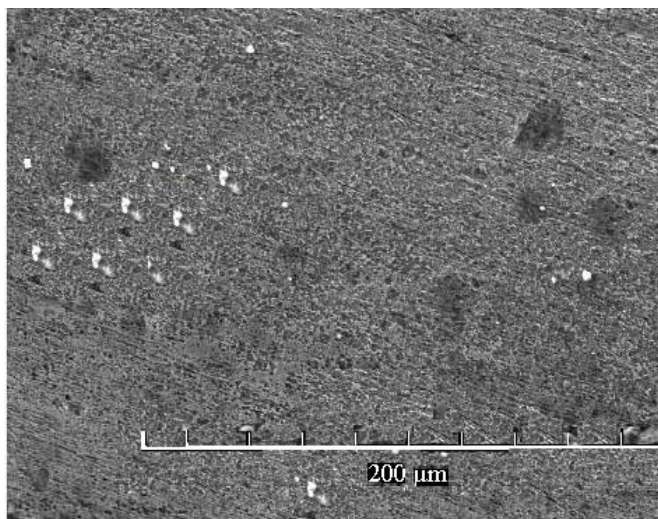


Fig. 8. SEM micrograph of the surface of VT-9 in 4 M sulfuric acid in the presence of 30 ppm L-SH at 303 ± 1 K.

trend of increasing inhibitor adsorption with an increase in temperature suggests the L-SH molecules are physically adsorbed in low concentrations, but are easily chemisorbed at high concentrations (30 ppm and above).

REFERENCES

- [1] L.J. Barron, Light Metal Age. 14 (1956) 16.
- [2] V.S. Ivins, Power Eng. 69 (1956) 52.
- [3] E. Leitao, R.A. Silva, M.A. Barbosa, Corros. Sci. 3 (1997) 337.
- [4] K. Elagli, M. Traisnel, H.F. Hildebrand, Electrochim. Acta 38 (1993) 1769.
- [5] Z. Han, H. Zhao, X.F. Chen, H.C. Lin, Mat. Sci. Eng. A-Struct. 277 (2000) 38.
- [6] R.S. Glass, Y. Ki Hong, Electrochim. Acta 29 (1984) 1465.
- [7] M.J. Mandry, G.J. Rosenblatt, J. Electrochem. Soc. 106 (1959) 755.
- [8] I. Gurrappa, Mater. Charac. 51 (2003) 131.
- [9] D.W. Deberry, G.R. Peyton, W.S. Clark, Corrosion. 40 (1981) 250.
- [10] E.E. Ebenso, Mater. Chem. Phys. 71 (2002) 62.

- [11] H. Ashassi-Sorkhabi, S.A. Nabavi-Amri, *Acta Chim. Slov.* 47 (2000) 587.
- [12] E.E. Oguzie, C. Unaegbu, C.E. Ogukwe, B.N. Okolue, A.I. Onuchukwu, *Mater. Chem. Phys.* 84 (2000) 364.
- [13] E.S. Ferreira, C. Giacomelli, F.C. Gicomelli, A. Spinelli, *Mater. Chem. Phys.* 83 (2004) 129.
- [14] I. Lukovists, E. Kalman, F. Zuchi, *Corrosion* 57 (2001) 3.
- [15] N. Hackerman, E.L. Cook, *J. Electrochem. Soc.* 97 (1950) 2.
- [16] E. Ahlberg, M. Friel, *Electrochim. Acta* 34 (1989) 190.
- [17] A.P. Brynza, L.I. Gerasytina, *J. Appl. Chem.* 35 (1962) 660.
- [18] L.I. Gerasytina, A.P. Brynza, *J. Appl. Chem.* 368 (1963) 2132.
- [19] J.A. Petit, G. Chatainier, F. Dabost, *Corros. Sci.* 21 (1981) 279.
- [20] V.B. Singh, S.M.A. Hosseini, *Corros. Sci.* 34 (1993) 1723.
- [21] V.B. Singh, S.M.A. Hosseini, *J. Appl. Electrochem.* 24 (1993) 250.
- [22] A.M. Al-Mayouf, A.A. AL-Swayih, N.A. Al-Mobarak, A.S. Al-Jabab, *Mater. Chem. Phys.* 86 (2004) 320.
- [23] S.M.A. Hosseini, V.B. Singh, *Mater. Chem. Phys.* 33 (1993) 63.
- [24] S. Bilgic, M. Sahin, *Mater. Chem. Phys.* 70 (2001) 290.
- [25] E.E. Ebenso, *Mater. Chem. Phys.* 71 (2002) 62.
- [26] A.M. Al-Mayouf, *Corros. Prevention Control* 6 (1996) 70.
- [27] M.P. Soriaga, A.T. Hubbard, *J. Electroanal. Chem.* 165 (1984) 79.
- [28] M.T. Makhlof, G.K. Gomma, M.H. Wahdan, Z.H. Khali, *Chem. Phys.* 40 (1995) 119.
- [29] A. Fragnani, G. Trabanelli, *Corrosion* 55 (1999) 653.
- [30] G.K. Gomma, M.H. Wahdan, *Bull. Chem. Soc. Jpn.* 67 (1994).
- [31] D.J. Shaw, *Introduction to Colloid and Surface Chemistry*, Butterworth, London, 1966.
- [32] D. Schlain, C.B. Kenahan, *Corrosion* 14 (1958) 405t.
- [33] G.W. Poling, *J. Electrochem. Soc.* 114 (1967) 1209.